

## Neutron diffraction and RMC modeling of new amorphous molybdate system

M Fabian<sup>1,2</sup>, E Svab<sup>2</sup>, K Krezhov<sup>3</sup>

<sup>1</sup>Centre for Energy Research, H-1525 Budapest P.O.B. 49, Hungary

<sup>2</sup>Wigner Research Centre for Physics, H-1525 Budapest P.O.B. 49, Hungary

<sup>3</sup>Institute for Nuclear Research and Nuclear Energy, 1784 Sofia, 72 Tzarigradsko Chaussee, Bulgaria

E-mail: [fabian.margit@energia.mta.hu](mailto:fabian.margit@energia.mta.hu)

**Abstract.** The network structure of boromolybdate  $\text{MoO}_3\text{-Nd}_2\text{O}_3\text{-B}_2\text{O}_3$  glasses has been investigated by neutron diffraction and reverse Monte Carlo (RMC) simulation technique. The partial atomic correlation functions, first neighbour atom distances and the coordination numbers have been revealed. Formation of  $\text{MoO}_4$  (55%) and  $\text{MoO}_6$  (45%) units was established for the binary  $90\text{MoO}_3\text{-10Nd}_2\text{O}_3$  glass. The ternary glasses consist from  $\text{MoO}_4$ ,  $\text{BO}_3$  and  $\text{BO}_4$  units. The relative number of  $\text{BO}_3$  is increasing with increasing boron content. Characteristic second neighbour distributions indicate the existence of a pronounced intermediate-range ordering through  $\text{MoO}_4\text{-BO}_4$  and  $\text{MoO}_4\text{-BO}_3$  linkages.

### 1. Introduction

Rare-earth molybdate phases exhibit a great variety of important physical properties including high ion and electron conductivity of fast oxide ion conductors, non-linear optical response and luminescent properties. In contrast to crystalline molybdates, the preparation and structural information on amorphous molybdate systems is far not well known.  $\text{MoO}_3$  is a conditional network former, it is not able to form a glass itself at even rapid cooling rates.

A systematic study to clear up the tendency for glass formation and immiscibility in the complex mixed boromolybdate glasses has been performed by Dimitriev et al. [1-5]. The phase diagram for  $\text{MoO}_3\text{-Nd(La)}_2\text{O}_3\text{-B}_2\text{O}_3$  was set up [3] and the basic structural and optical characteristics were investigated by XRD, DTA, SEM, UV-VS spectra and IR spectroscopy [5]. The  $\text{Nd}_2\text{O}_3$  is an appropriate component due to its specific optical properties but it increases the melting temperature, while by adding  $\text{B}_2\text{O}_3$  it is possible to obtain low melting materials in a relatively wide concentration range.

In order to get a deeper insight into the network structure of  $\text{MoO}_3\text{-Nd}_2\text{O}_3\text{-B}_2\text{O}_3$  glassy system, we have undertaken a neutron diffraction study combined with reverse Monte Carlo (RMC) computer simulation technique [6]. We expect to obtain new structural characteristics of the partial atomic pair correlation functions, especially on the first neighbour atomic distances, coordination numbers and network former units and their linkages.



## 2. Experimental details and methods

### 2.1. Samples

The amorphous materials have been prepared by a conventional melt quenching method. The nominal compositions of the studied glasses are binary 90MoO<sub>3</sub>-10Nd<sub>2</sub>O<sub>3</sub> and ternary 50MoO<sub>3</sub>-25Nd<sub>2</sub>O<sub>3</sub>-25B<sub>2</sub>O<sub>3</sub>, 40MoO<sub>3</sub>-30Nd<sub>2</sub>O<sub>3</sub>-30B<sub>2</sub>O<sub>3</sub>, 20MoO<sub>3</sub>-30Nd<sub>2</sub>O<sub>3</sub>-50B<sub>2</sub>O<sub>3</sub> (mol%). Commercial powder of reagent grade MoO<sub>3</sub>, Nd<sub>2</sub>O<sub>3</sub> and B<sub>2</sub>O<sub>3</sub> were used as starting materials and were mixed in an alumina mortar. B<sub>2</sub>O<sub>3</sub> was isotopically enriched in <sup>11</sup>B (99.6%) in order to reduce the influence of the high neutron absorption of <sup>10</sup>B present in natural boron. For the details of sample preparation we refer to [3,5].

### 2.2. Neutron diffraction experiments

Neutron diffraction (ND) measurements have been performed by the PSD diffractometer ( $\lambda_0=1.068$  Å) [7] at the 10 MW Budapest research reactor and by the 7C2 diffractometer at the LLB-CEA-Saclay ( $\lambda_0=0.726$  Å) [8], the powder specimens of about 3–4 g/each were filled in thin walled cylindrical vanadium sample holder of 8 mm and 6 mm diameter, respectively. Data were corrected for detector efficiency and background scattering. The total structure factor,  $S(Q)$  was calculated as described in our previous work [9]. Figure 1 shows the experimental  $S(Q)$  data for the investigated samples together with the results of RMC simulation (details of the RMC modeling will be discussed in the next section).

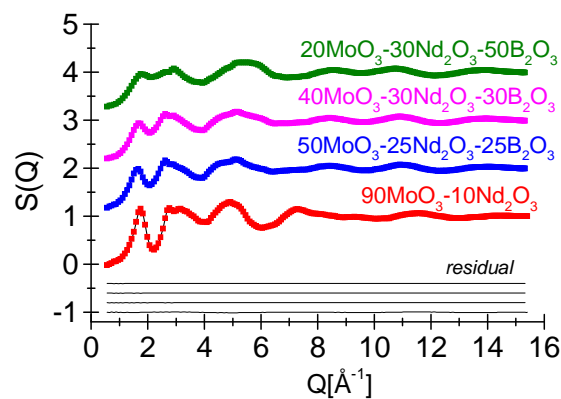


**Figure 1.** Structure factor of the boromolybdate glasses: experimental data (marks) and RMC simulation (solid line). The residuals of the experimental  $S_{\text{EXP}}(Q)$  and calculated  $S_{\text{RMC}}(Q)$  are shown at the bottom of the figure. (The curves are shifted vertically for clarity)

The overall run of the  $S(Q)$  data for the binary 90MoO<sub>3</sub>-10Nd<sub>2</sub>O<sub>3</sub> glass is fairly different from those of the ternary glasses containing network former B<sub>2</sub>O<sub>3</sub>. The most striking feature is the relatively high intensity and sharp distribution of the first peak of the binary glass, which is a fingerprint of a short-range network structure, i.e. formation of well-defined units. For the ternary glasses the intensity of the first peak decreases, gets broader and slightly shifts to higher values with increasing boron content. This indicates a more complex network structure of the ternary glasses in comparison to the binary glass, as it can be expected. The second peak contains two small humps, the average main intensity changes in dependence of concentration. The third peak gets significantly broader for the ternary glasses and, for the higher order oscillations, above  $Q \geq 6$  Å<sup>-1</sup> phase displacement can be observed.

### 2.3. Reverse Monte Carlo simulation

The experimental  $S(Q)$  data have been simulated by the RMC method [6] using the software package [10]. The RMC minimizes the squared difference between the experimental  $S(Q)$  and the calculated one from a 3-dimensional atomic configuration. The RMC algorithm calculates the one-dimensional partial atomic pair correlation functions  $g_{ij}(r)$ , for details we refer here to our previous work [9].

In this study for the RMC starting model a disordered atomic configuration was built up with a simulation box containing 10 000 atoms. In the calculations, density values 0.0673, 0.0683, 0.0684 and 0.0692 atoms·Å<sup>-3</sup> were used [11] for the 90MoO<sub>3</sub>-10Nd<sub>2</sub>O<sub>3</sub>, 50MoO<sub>3</sub>-25Nd<sub>2</sub>O<sub>3</sub>-25B<sub>2</sub>O<sub>3</sub>, 40MoO<sub>3</sub>-30Nd<sub>2</sub>O<sub>3</sub>-30B<sub>2</sub>O<sub>3</sub> and 20MoO<sub>3</sub>-30Nd<sub>2</sub>O<sub>3</sub>-50B<sub>2</sub>O<sub>3</sub> samples, respectively, and the corresponding RMC half-box lengths were 26.483, 26.353, 26.340 and 26.238 Å.

In the RMC simulation procedure two types of constraints were used: the minimum interatomic distances between atom pairs (cut-off distances) and connectivity constraints for Mo-O and for B-O atom pairs. Molybdenum atoms were restricted to be surrounded by 4 or 6 oxygen atoms, as suggested in previous studies [3,12]. For the B-O coordination we supposed the formation of trigonal BO<sub>3</sub> and tetrahedral BO<sub>4</sub> units, which has been reported in several works, i.e. for binary neodymium borate glasses [13], for ternary rare-earth boromolybdate MoO<sub>3</sub>-Nd(La)<sub>2</sub>O<sub>3</sub>-B<sub>2</sub>O<sub>3</sub> [3-5], for B<sub>2</sub>O<sub>3</sub>-Bi<sub>2</sub>O<sub>3</sub>-MoO<sub>3</sub> glass [14], and for binary alkali borate glasses [15,16]. In the RMC calculations boron atoms were forced to have 3 or 4 oxygen neighbours in the interval 1.2-1.7 Å, the upper limit was used not to overlap with Mo-O distribution.

The starting cut-off distances have been taken from the literature based on the results of crystalline compounds [17] and from glassy systems [18,19] of similar compositions. Several RMC runs have been performed by modifying slightly the cut-off distances for the various atom pairs. The convergence of the RMC simulation was good, the set of cut-off distances used in the final RMC run are the following: B-O 1.2 Å; Mo-O 1.71 Å; O-O 2.3 Å; Nd-O 2.37 Å; B-B 2.36 Å; Nd-Nd 2.65 Å; Mo-B 2.7 Å; Nd-B 3.05 Å; Mo-Mo 3.1 Å; Mo-Nd 3.45 Å.

### 3. Results and discussion

The calculated  $S_{\text{RMC}}(Q)$ s matched very well the experimental  $S_{\text{EXP}}(Q)$ s for all compositions, as it is illustrated in figure 1. The partial correlation functions,  $g_{ij}(r)$  and coordination numbers were revealed from the RMC modeling. Here we focus on the results obtained for the network former Mo-O and B-O correlations.

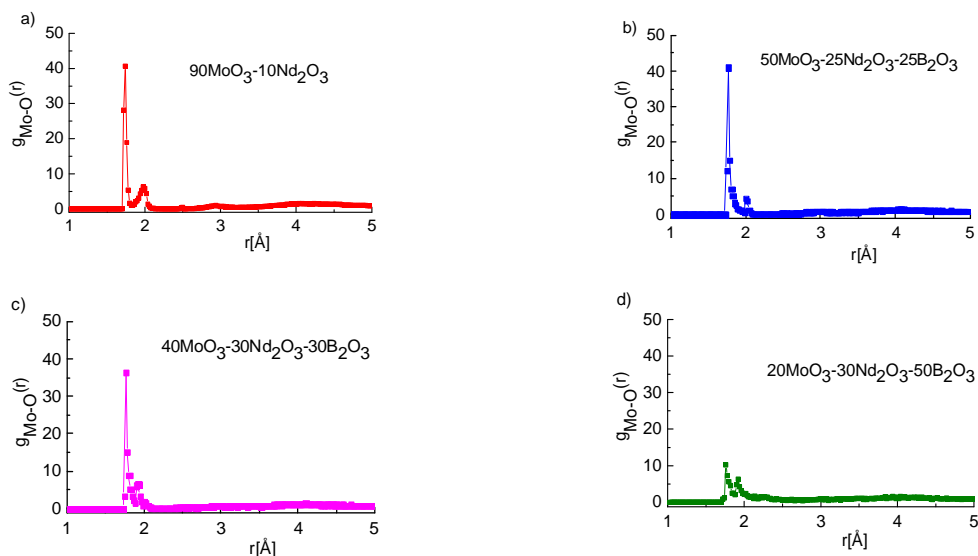


**Figure 2.** The Mo-O partial atomic pair correlation functions from RMC modeling.

Figure 2 shows the Mo-O correlation functions. For all compositions the first neighbour distributions show a sharp peak at  $1.75 \pm 0.02 \text{ \AA}$  with a half-width value of  $0.04 \text{ \AA}$ , while a significantly smaller “sub”-peak appears at  $1.95 \pm 0.05 \text{ \AA}$ . For  $90\text{MoO}_3\text{-}10\text{Nd}_2\text{O}_3$  sample the intensity of both peaks is high, and the statistics is good due to the high weighting factor,  $w_{\text{Mo-O}}=33.79\%$ . The “sub”-peak at  $1.98 \text{ \AA}$  is significantly broader than the first peak, the half-width value is  $0.08 \text{ \AA}$ . With decreasing Mo-content the intensity of the first neighbour peak intensity decreases. The distributions for  $50\text{MoO}_3\text{-}25\text{Nd}_2\text{O}_3\text{-}25\text{B}_2\text{O}_3$  and  $40\text{MoO}_3\text{-}30\text{Nd}_2\text{O}_3\text{-}30\text{B}_2\text{O}_3$  samples are very similar due to the small difference in the compositions. The position of the small “sub”-peaks is slightly shifted (by  $0.1 \text{ \AA}$ ), which is within limit of error. For the  $20\text{MoO}_3\text{-}30\text{Nd}_2\text{O}_3\text{-}50\text{B}_2\text{O}_3$  sample, even the intensity of the main Mo-O peak at  $1.75 \text{ \AA}$  is fairly small, due to the small amount of molybdenum in this sample.

The average coordination number for the binary  $90\text{MoO}_3\text{-}10\text{Nd}_2\text{O}_3$  sample is  $CN_{\text{Mo-O}}=4.9 \pm 0.2$  atoms. If we suppose that  $\text{MoO}_4$  and  $\text{MoO}_6$  units are present in the network, it would mean that 55% of the Mo atoms are 4-fold oxygen coordinated, while 45% are 6-fold coordinated. Taking into consideration the  $g_{\text{Mo-O}}(r)$  distribution, we can establish that the shorter distance at  $1.74 \text{ \AA}$  can be attributed to the  $\text{MoO}_4$  units, while in addition two further oxygen neighbours appear at a longer  $1.98 \text{ \AA}$  distance forming  $\text{MoO}_6$  units.

For the ternary  $50\text{MoO}_3\text{-}25\text{Nd}_2\text{O}_3\text{-}25\text{B}_2\text{O}_3$  and  $40\text{MoO}_3\text{-}30\text{Nd}_2\text{O}_3\text{-}30\text{B}_2\text{O}_3$  samples the average coordination number, as calculated from the RMC modeling, is  $CN_{\text{Mo-O}}=4.2$  and  $4.0 \pm 0.2$  atoms, respectively. As far as, the corresponding  $g_{\text{Mo-O}}(r)$  distributions contain a small “sub”-peak at  $1.95 \text{ \AA}$ , we may conclude that 95% of the Mo atoms form  $\text{MoO}_4$  units, while about 5% form  $\text{MoO}_6$  units. For the  $20\text{MoO}_3\text{-}30\text{Nd}_2\text{O}_3\text{-}50\text{B}_2\text{O}_3$  sample the average coordination number is  $CN_{\text{Mo-O}}=3.5 \pm 0.3$  atoms, which is less than the expected 4-fold coordination. This may be the consequence of the relatively large error due to the relatively small amount of molybdenum leading to a low value of the weighting factor  $w_{\text{Mo-O}}=5.57\%$ , however, distortion of the tetrahedral  $\text{MoO}_4$  units can not be excluded.

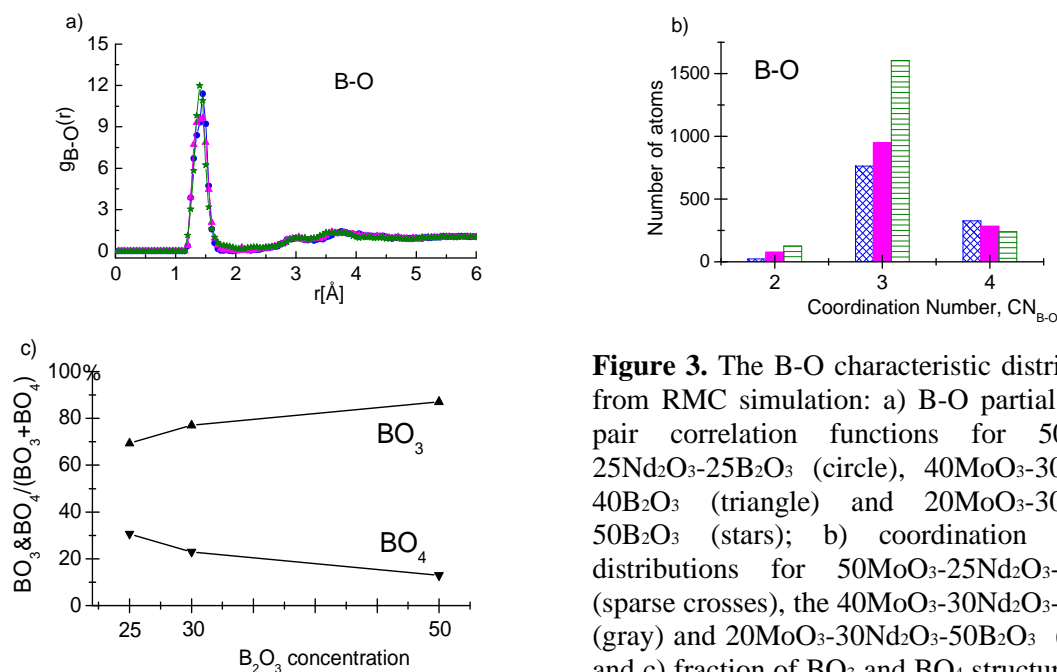


**Figure 3.** The B-O characteristic distributions from RMC simulation: a) B-O partial atomic pair correlation functions for  $50\text{MoO}_3\text{-}25\text{Nd}_2\text{O}_3\text{-}25\text{B}_2\text{O}_3$  (circle),  $40\text{MoO}_3\text{-}30\text{Nd}_2\text{O}_3\text{-}40\text{B}_2\text{O}_3$  (triangle) and  $20\text{MoO}_3\text{-}30\text{Nd}_2\text{O}_3\text{-}50\text{B}_2\text{O}_3$  (stars); b) coordination number distributions for  $50\text{MoO}_3\text{-}25\text{Nd}_2\text{O}_3\text{-}25\text{B}_2\text{O}_3$  (sparse crosses), the  $40\text{MoO}_3\text{-}30\text{Nd}_2\text{O}_3\text{-}40\text{B}_2\text{O}_3$  (gray) and  $20\text{MoO}_3\text{-}30\text{Nd}_2\text{O}_3\text{-}50\text{B}_2\text{O}_3$  (sparse) and c) fraction of  $\text{BO}_3$  and  $\text{BO}_4$  structural units as a function of concentration.

Figure 3 shows the characteristics for the B-O correlations. The first neighbour distributions show a relatively broad – in comparison to the Mo-O distribution - first neighbour distance at  $1.40 \pm 0.02 \text{ \AA}$  with a half-width value of  $0.25 \text{ \AA}$ , and they practically overlap for the three ternary  $\text{MoO}_3\text{-Nd}_2\text{O}_3\text{-B}_2\text{O}_3$  glasses of different concentrations within limit of error as it is shown in figure 3/a. Figure 3/b

illustrates the B-O coordination number distributions, which contain both 3- and 4-fold oxygen coordinated boron atoms (the small number of 2-neighbours is probably an artificial effect of RMC calculation). The average coordination numbers slightly decreases from 3.3 to 3.1 atoms with increasing boron content. The fraction of  $\text{BO}_3$  and  $\text{BO}_4$  to the total number of  $\text{BO}_3+\text{BO}_4$  is an important structural characteristic. It was found that it depends on the boron concentration, as it is illustrated in figure 3/c. With increasing boron content the relative number of  $\text{BO}_3$  units is increasing, while the number of  $\text{BO}_4$  is decreasing. For  $50\text{MoO}_3\text{-}25\text{Nd}_2\text{O}_3\text{-}25\text{B}_2\text{O}_3$  sample  $\sim 70\%$  of B-atoms are 3-coordinated, while  $\sim 30\%$  are 4-coordinated, the average coordination number is 3.3 atoms; for  $40\text{MoO}_3\text{-}30\text{Nd}_2\text{O}_3\text{-}30\text{B}_2\text{O}_3$  glass  $\sim 77\%$  of B-atoms are 3-coordinated, while  $\sim 23\%$  are 4-coordinated, the average coordination number is 3.2 atoms; for  $20\text{MoO}_3\text{-}30\text{Nd}_2\text{O}_3\text{-}50\text{B}_2\text{O}_3$  sample  $\sim 87\%$  of B-atoms are 3-coordinated, while  $\sim 13\%$  are 4-coordinated, the average coordination number is 3.1 atoms.

In the studied system the results obtained from RMC modeling have shown significant correlations between several second neighbour atom pairs, as it is shown in figure 4. This is important, as far as the analysis of these results may give useful information on the linkage of the basic structural units forming the network structure. The linkage between the  $\text{MoO}_4$  units leads to the Mo-Mo correlation distance at 3.2 Å. The second neighbour distances for B-B are obtained at 2.4 Å, for Mo-B at 2.8 Å, which indicate mixed linkages, and for Nd-B at 3.1 Å. These results indicate the existence of a pronounced intermediate-range ordering.

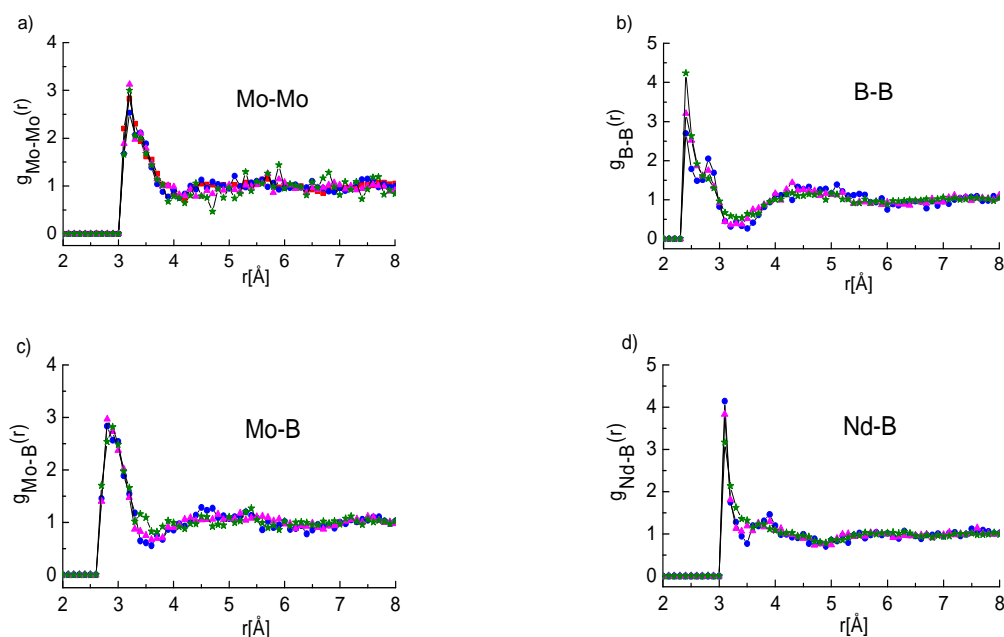


**Figure 4.** Second neighbour partial atomic pair correlation functions obtained from the RMC modeling for the boromolybdate glasses: a) Mo-Mo b) B-B c) Mo-B and d) Nd-B, where  $90\text{MoO}_3\text{-}10\text{Nd}_2\text{O}_3$  (square),  $50\text{MoO}_3\text{-}25\text{Nd}_2\text{O}_3\text{-}25\text{B}_2\text{O}_3$  (circle),  $40\text{MoO}_3\text{-}30\text{Nd}_2\text{O}_3\text{-}40\text{B}_2\text{O}_3$  (triangle) and  $20\text{MoO}_3\text{-}30\text{Nd}_2\text{O}_3\text{-}50\text{B}_2\text{O}_3$  (stars).

#### 4. Conclusions

Neutron diffraction study has been performed on binary  $90\text{MoO}_3\text{-}10\text{Nd}_2\text{O}_3$  and ternary  $\text{MoO}_3\text{-Nd}_2\text{O}_3\text{-B}_2\text{O}_3$  glasses prepared by melt quench technique. The network structure was modeled by reverse Monte Carlo simulation method. From the RMC modeling the partial atomic correlation functions and the coordination numbers have been revealed. Our main findings are the following:

- in the binary glass  $\text{MoO}_4$  (55%) and  $\text{MoO}_6$  (45%) structural units were revealed;
- in ternary system mainly  $\text{MoO}_4$  units are present, and with decreasing  $\text{MoO}_3$  concentration, the ratio of  $\text{MoO}_6$  units roughly decreases;

- in the ternary glasses the B-O network is formed by  $\text{BO}_3$  and  $\text{BO}_4$  groups, and with increasing  $\text{B}_2\text{O}_3$  content conversion of  $\text{BO}_4$  to  $\text{BO}_3$  takes place;
- in ternary system pronounced intermediate range order exists, which indicates mixed  $\text{MoO}_4$ - $\text{BO}_4$  and  $\text{MoO}_4$ - $\text{BO}_3$  linkages.

**Acknowledgement** - The authors are grateful to Dr. L. Alexandrov for sample preparation and for helpful discussions. The research was supported by the EU-FP7-NMI3 No.283883. Thanks to the financial support of Hungarian OTKA-PD 109384 and to the bilateral cooperation of Hungarian-Bulgarian Academy of Sciences SNK-63/2013.

## References

- [1] Alexandrov L, Iordanova R, Dimitriev Y, Hamda K, Ide J and Milanova M 2008 *Advanced Materials Research* **39-40** 37
- [2] Aleksandrov L, Iordanova R and Dimitriev Y 2007 *Phys. Chem. Glasses: European J. Glass Sci. Technol. B.* **48** 242
- [3] Aleksandrov L, Iordanova R and Dimitriev Y 2009 *Journal of Non-Crystalline Solids* **355** 2023
- [4] Dimitriev Y, Iordanova R, Aleksandrov L and Kostov K L 2008 *Phys. Chem. Glasses Eur/ Glass Sci. Technol B.* **50** 218
- [5] Aleksandrov L, Komatsu T, Iordanova R and Dimitriev Y 2011 *Journal of Physics and Chemistry of Solids* **72** 263
- [6] McGreevy R L and Pusztai L 1988 *Mol. Simul.* **1** 359
- [7] Sváb E, Mészáros Gy and Deák F 1996 *Materials Science Forum* **228** 247; <http://www.bnc.hu/>
- [8] Ambroise J P, Bellissent R 1984 *Rev. Phys. Appl.* **19** 731; <http://www-llb.cea.fr/en/>
- [9] Fábrián M, Sváb E, Proffen Th and Veress E 2008 *Journal of Non-Crystalline Solids* **354** 3299
- [10] <http://www.szfki.hu/~nphys/rmc++/opening.html>
- [11] Alexandrov L, private communication
- [12] Rada M, Rada S, Pascuta P and Culea E 2010 *Spectrochimia Acta Part A* **77** 832
- [13] Burns A E, Winslow D W, Clarida W J, Affatigato M, Feller S A and Brow R K 2006 *Journal of Non-Crystalline Solids* **352** 2364
- [14] Iordanova R, Aleksandrov L, Bachvarova-Nedelcheva A, Ataala M and Dimitriev Y 2011 *Journal of Non-Crystalline Solids* **357** 2663
- [15] Fábrián M, Sváb E, Proffen Th and Veress E 2010 *Journal of Non-Crystalline Solids* **356** 441
- [16] Wright A C, Sinclair R N, Stone C E and Shaw J L 2012 *Phys. Chem. Glasses Eur. J. Glass Sci. Technol.* **B53** 191
- [17] Barker R S and Evans I R 2006 *Journal of Solid State Chemistry* **179** 1918
- [18] Wang H, Peng J, Chen D F and Hu Z 2006 *Solid State Sciences* **8** 1144
- [19] Wang Z, Zhang L, Wang G, Song M, Huang Y and Wang G 2009 *Optical Materials* **31** 849